

Radiation Losses of the Dominant Mode in Round Dielectric Waveguides

By DIETRICH MARCUSE

(Manuscript received March 5, 1970)

The radiation loss theory that has been developed in a series of earlier papers is extended to the dominant mode of the round dielectric waveguide. The theory is applied to the calculation of radiation losses of abrupt steps, gradual tapers, and random wall perturbations of the round dielectric waveguide.

The radiation losses caused by an abrupt step, and consequently the losses of tapers, are far higher for the dominant mode of the round dielectric waveguide than they are for corresponding steps and tapers of the dielectric slab waveguide. However, the losses caused by infinitesimal random wall perturbations of the round waveguide are nearly equal to the random wall losses predicted on the basis of the slab waveguide theory. In fact the losses of the dominant mode as well as the circular electric TE_{01} mode of the round rod due to random wall perturbations are very nearly the same.

The theory is limited to circular symmetric distortions of the round dielectric rod (diameter changes). The radiation losses caused by steps of the round dielectric waveguide that carries the dominant guided mode have been verified by experiments at millimeter wave frequencies.

I. INTRODUCTION

A series of earlier papers was devoted to radiation losses of TE and TM modes in dielectric slab waveguides.¹⁻³ The radiation losses were assumed to be caused either by random perturbations of the waveguide boundary¹ or by steps and tapers of the slab waveguide.³ Experiments to verify the radiation loss theory were conducted with millimeter waves in round teflon rods, and the theory was extended to cover this case.²

These earlier publications were limited to the simplified case of

electromagnetic fields that are independent of one coordinate. In the case of the slab waveguide we assumed

$$\frac{\partial}{\partial y} = 0 \quad (1)$$

while

$$\frac{\partial}{\partial \phi} = 0 \quad (2)$$

was required of the fields of the round dielectric waveguide. Restrictions (1) and (2) made it possible to separate the fields into transverse electric (TE) or transverse magnetic (TM) modes.

The study of the simple slab waveguide yielded much useful information about the general properties of radiation losses and allowed us to infer the order of magnitude of the radiation losses caused by random wall imperfections. However, the dielectric slab is not a useful practical waveguide and can be used only as a simplified model to obtain information about the behavior of more realistic and more complicated structures. Limitation (2) for the modes of the realistic and practical round dielectric waveguide precludes the application of the theory to the most important dominant mode of this structure.

The present paper is devoted to a study of the radiation losses of the dominant mode of the round dielectric waveguide (optical fiber). To be able to handle the theory we still impose condition (2) on the derivatives related to the geometry of the waveguide but not on the field distribution. The resulting theory is still very complicated so that we must limit ourselves to sketching the theory and stating the final results.

The radiation losses caused by random imperfections [obeying restriction (2)] are very nearly identical to the losses of the corresponding slab waveguide problem. However, the radiation losses of the dominant mode caused by steps and tapers in the waveguide are much higher than the corresponding losses of the TE or TM modes in the slab waveguide. The radiation losses of the dominant mode due to waveguide steps have been found experimentally to be in agreement with the theory.

In order to allow the reader to obtain the information concerning the results of the theory unencumbered by complex mathematical formulas we start the paper with a discussion of the results. The remainder of the paper is devoted to an outline of the theory that was used to obtain these results.

II. NUMERICAL AND EXPERIMENTAL RESULTS

2.1 *Radiation Losses of Waveguide Steps*

We begin the discussion of the consequences of the radiation loss theory of the dominant mode of the round dielectric waveguide by considering the radiation losses caused by the abrupt step of the waveguide diameter shown in Fig. 1. As described in Section II, the radiation losses caused by an abrupt step can be calculated by two different methods. The mode matching technique infers the loss from the transmission coefficient of the guided mode that continues to travel in the waveguide after it has passed the step. The radiation loss method accounts for the lost power by directly calculating the amount of power radiated into space. Both methods involve approximations so that we cannot expect to obtain exactly the same results either way.

Figure 2 shows the results of both methods of calculation. The radiation loss caused by a step with $a_2/a_1 = 0.5$ as a function of ka_1 (as computed by means of the mode matching technique) is shown as the dotted line in the figure, while the solid line represents the result of the radiation loss method. The curve holds for a dielectric rod with index of refraction $n = 1.432$ ($n^2 = 2.05$). This index was chosen since it is representative of teflon at a frequency of 55 GHz. The agreement of the two methods is remarkably good considering the approximations involved in deriving the theoretical expressions.

Even better agreement is obtained by a similar calculation that applies to a dielectric rod with index of refraction $n = 1.01$ as shown in Fig. 3. Both figures are extended over ka_1 values that correspond to single guided mode operation. There are other guided modes possible over part of the range of ka_1 values but these other modes do not couple to the dominant mode of the round dielectric rod because of the restriction on symmetry imposed by equation (2). It is in this sense that the operation of the waveguide is single mode. No other guided mode occurs under the imposed conditions. The shape of the two curves in Figs. 2

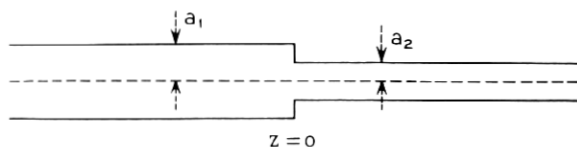


Fig. 1—Step in the round dielectric waveguide.

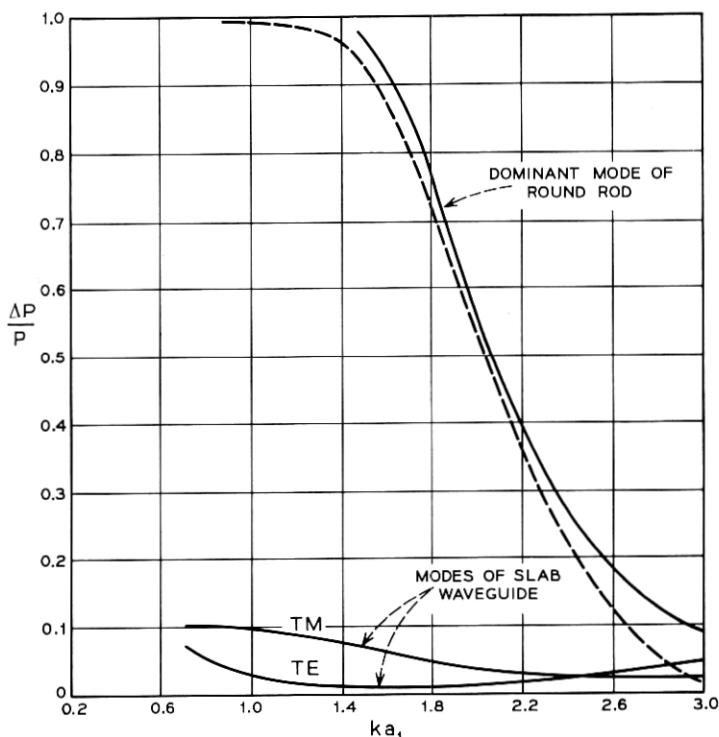


Fig. 2—Relative radiation loss caused by an abrupt step with $a_2/a_1 = 0.5$ of the waveguide. The two curves labeled dominant mode of the round waveguide were obtained by the mode matching technique (dotted line) and by the radiation loss technique (solid line). The two curves at the bottom of the figure labeled TE and TM modes represent the step losses of the slab waveguide. The radius a_1 (appearing in ka_1) belongs to the larger waveguide section. Index of refraction $n = 1.432$.

and 3 is very similar. Both curves reach into high loss regions for small values of ka_1 . The curve of Fig. 3 is applicable to a clad optical fiber with 1 percent index difference between core and cladding. The curves shown on the bottom of Figs. 2 and 3 represent the step losses of TE and TM modes of the slab waveguide.³ These curves are computed for the same index of refraction. The dimension a_1 (of ka_1) is the half width of the slab in the case of the slab waveguide. It is striking how much lower the radiation losses of the guided modes of the slab waveguide are compared to the dominant mode of the round dielectric rod.

Because of the complexity of the theory and because the step loss results are so different for the round rod and the slab waveguide, it

appeared desirable to confirm the loss predictions of the theory with an experiment. The experiment was conducted with millimeter waves (approximately 55 GHz). A round teflon rod of 0.191 cm diameter was mounted between two metallic reflectors as shown in Fig. 4. The resulting resonant cavity could be excited through small holes in the reflector plates that, simultaneously, acted as supports for the teflon rod. Two teflon sleeves of 0.216 cm and 0.242 cm outer diameter could be slid over the teflon rods to produce a round dielectric waveguide with two steps. The losses caused by the steps could be determined from Q measurements of the cavity with and without the teflon sleeves. The results of these loss measurements (applied to one step) are shown as crosses in Fig. 5. This figure also shows the theoretical loss predictions of the mode matching (dotted line) and the radiation loss approach (solid line) of the theory. Note that the parameter value $ka_2 = 1.1$ of this figure uses the fixed value of the narrower portion of the waveguide as reference.

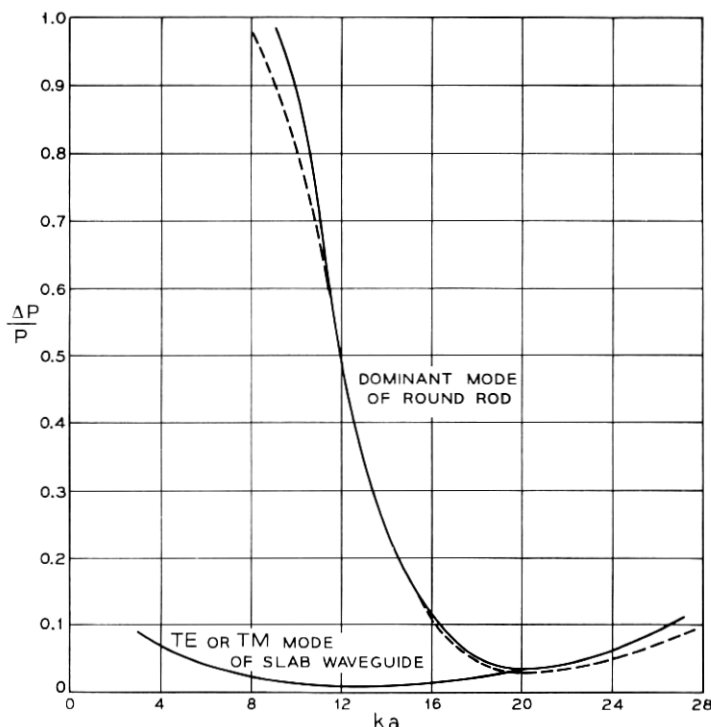


Fig. 3—This curve is similar to Fig. 2 with $n = 1.01$ and $a_2/a_1 = 0.5$.

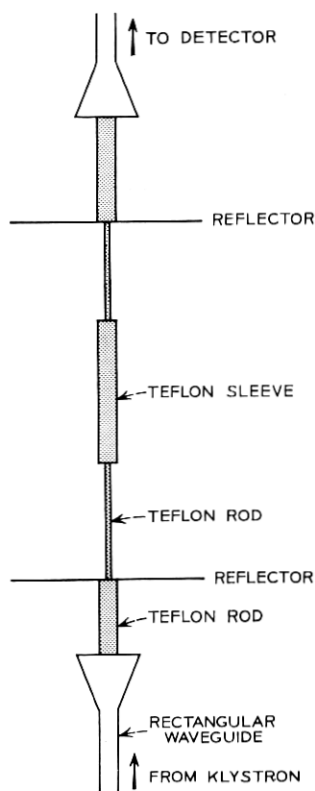


Fig. 4—Experimental resonant cavity set up to measure radiation losses of waveguide steps.

The point $a_2/a_1 = 0.5$ of Fig. 5 corresponds to the point $ka_1 = 2.2$ of Fig. 2. The measurements support the result of the round rod theory. The radiation losses of the slab waveguide even for much larger steps are still far lower than the measured values of these smaller steps of the round rod.

It is not as easy to confirm the loss predictions of the slab theory since a dielectric slab waveguide is somewhat of an idealization. In particular it is hard to excite a slab with a mode that has no field variation in the y -direction. In order to obtain some approximation to the slab waveguide we constructed a dielectric (teflon) ribbon whose dimensions on the narrower portion were 0.380 by 0.095 cm and whose wider dimensions were 0.380 by 0.190 cm. Note that only the narrow side is affected by the step. The losses of this ribbon waveguide with a 2:1 step were measured in the same resonant setup and compared to

the losses of a smooth ribbon with dimensions 0.380 by 0.095 cm. The radiation loss of the ribbon guide was $\Delta P/P = 0.08$ for $kd_2 = 1.1$ (or $kd_1 = 2.2$). This radiation loss value is shown as the circle in Fig. 5. It is apparent that the loss of the ribbon guide is far smaller than the loss of the round waveguide. It is about four times higher than the step loss predicted for the slab waveguide. However, we must keep in mind that the ribbon is only a poor approximation of the slab waveguide. It is therefore not surprising that its radiation loss cannot be predicted by the slab waveguide theory. The slab waveguide apparently can tolerate steps in its width exceptionally well.

2.2 Radiation Loss of Tapers

The radiation loss theory that is presented in the theoretical part can be used to determine the loss of round dielectric waveguides with

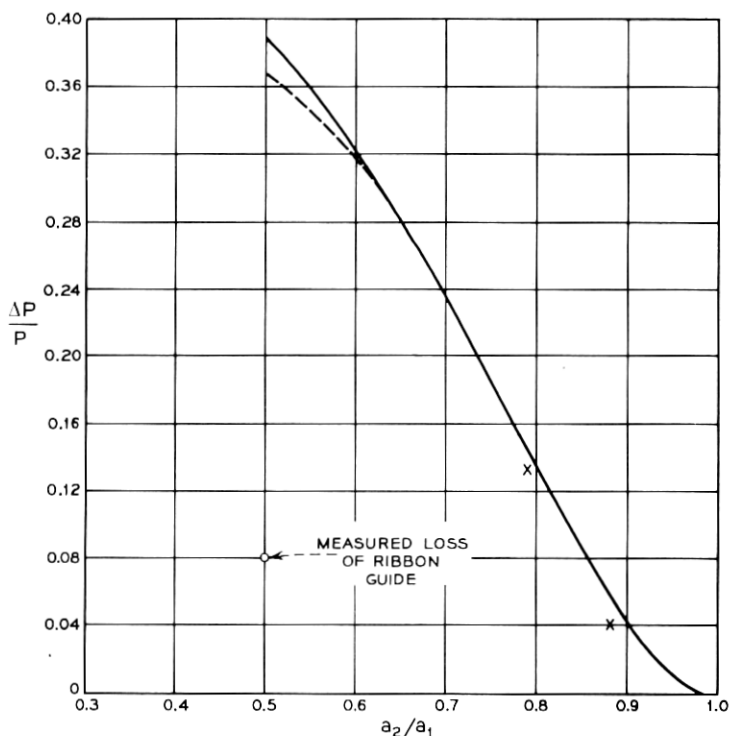


Fig. 5—Comparison of theory and experiment. The crosses are measured step losses of the round dielectric waveguide. The circle is the step loss of a ribbon guide. The curves represent the results of the mode matching theory (dotted line) and the radiation loss theory (solid line). ($n = 1.432$, $ka_2 = 1.1$.) Note that the curve parameter ka_2 uses the radius of the smaller waveguide section.

arbitrary diameter changes. Since the radiation losses of an abrupt step are very high for round dielectric waveguides it is interesting to study the radiation losses of gradual tapers.^{6,7}

The calculation of the radiation losses of tapers can be simplified by observing that the dependence of β_0 on the radius of the waveguide is nearly linear over a considerable range of values. Figure 6 shows the ratio of β_0/k as a function of ka for $n = 1.432$. It is apparent that a straight line approximation is possible in the region $1.2 < ka < 2.5$.

We study the radiation losses of two different tapers. The linear taper is the simplest and therefore the most reasonable taper to investigate. However, there are reasons to suspect that the linear taper may have higher radiation losses than other forms of tapers. It is apparent from equation (36) of Section II that the result of the integration (aside from the complicated factor $I(\rho, z)$ which is difficult to evaluate) depends on the product of the derivative of the radius function $a(z)$ with sine and cosine functions of the form $\int_0^z [\beta_0(z) - \beta] dz$. (β_0 is the propagation constant of the guided mode; β is the z -component of the propagation constant of the radiation modes.) The oscillatory function has the tendency to cancel contributions from those functions that appear multiplied with it under the integrand. The more rapidly the cosine function oscillates, the more effective will be its canceling influence.

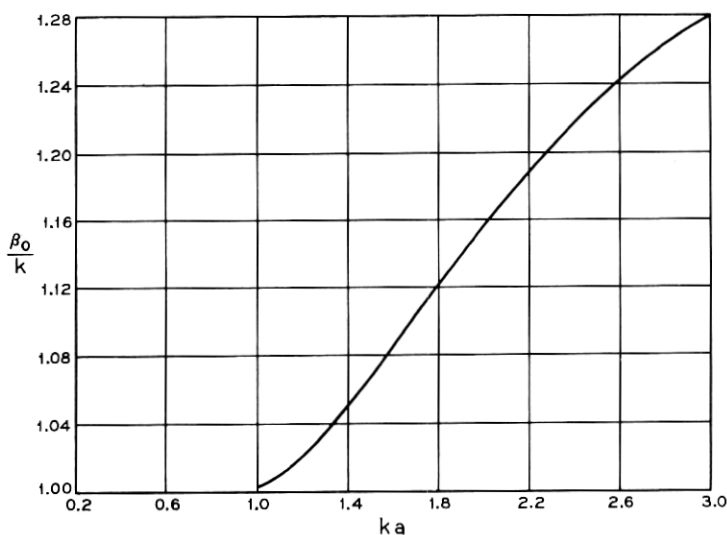


Fig. 6—Plot of the propagation constant β_0 of the dominant mode of the round dielectric waveguide. ($n = 1.432$.)

This consideration shows that we would like to see the values of $\beta_0(z) - \beta$ as large as possible. The smallest possible value, and consequently the most harmful, is the value $\beta_0(z) - k$ that is assumed at the upper end of the integration range in equation (34). However, because of the z dependence of β_0 the values of $\beta_0(z) - k$ are smaller at the narrow portion of the taper than they are on its wider portion. One might expect, therefore, that the narrow region of the linear taper contributes more to the overall radiation loss than its wider portions. It appears that the taper could be optimized if larger values of da/dz appeared at the wider end of the taper where the canceling effect of the sinusoidal functions is still more effective. Following this idea, it is possible to show that an exponential taper should distribute the radiation loss more evenly over its entire length in comparison with the linear taper. A linear taper and an exponential taper are shown in Fig. 7. The exponential taper was calculated from

$$a(z) = a_2 + (a_1 - a_2) \exp\left(-4.6 \frac{z}{L}\right).$$

This taper is designed to equalize the contribution of the integral (36), at least approximately, over the entire length of the taper assuming that $I(\rho, z)$ is constant. The discontinuity of da/dz at $z = 0$ does not contribute to the radiation loss. It would, therefore, be of no advantage to shape the taper such that da/dz is continuous over its entire length.

The radiation losses of the linear and exponential tapers are compared in Fig. 8. Even though the radiation loss of the exponential taper is less than that of the linear taper, in agreement with our expectation, the amount of improvement is insufficient to warrant the greater complexity required to produce such a more complicated taper. Figure 8 also shows that the radiation loss of a taper is far less than the losses caused by an abrupt step. The radiation losses can be made as small as desired with a taper of sufficient length. A linear taper with a length to waveguide radius (on the larger portion of the guide) ratio of $L/a_1 = 400$ reduces the radiation losses, that would occur on an abrupt step, by a factor of 100. With $\lambda = 1 \mu\text{m}$ the value $ka_1 = 2.5$ is realized for $a_1 = 0.4 \mu\text{m}$ so that the taper would have an actual length of $L = 160 \mu\text{m}$ or 0.16 mm. It is apparent that much longer, more effective tapers are feasible.

Figure 8 indicates that there are two distinctly different regions. Below $L/a_1 = 2$ the taper is so short that it acts like an abrupt step. The beneficial effect of the taper makes itself felt only if the taper is long enough. The reduction of the radiation loss of a gradual taper

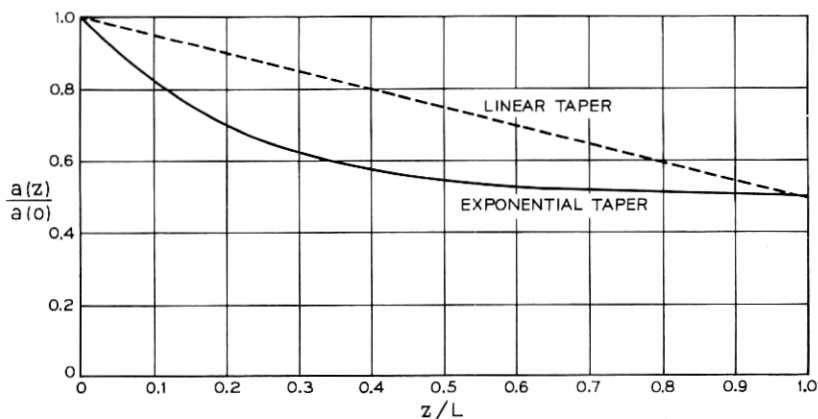


Fig. 7—The profile of the linear (dotted line) and the exponential (solid line) taper.

compared to an abrupt step or steep taper is caused by the canceling influence of the (complex) exponential function in the integral of equation (36).

2.3 Losses Caused by Random Wall Imperfections

An important loss contribution is caused by the random deviations of the dielectric waveguide boundary from perfect straightness. These radiation losses have been investigated for the slab waveguide¹ and for the circular electric TE_{01} mode.² The theory of radiation losses of the dominant mode of the round dielectric waveguide is sketched in Section III.

We have seen that the radiation losses caused by arbitrary deformations of the waveguide wall can be computed by describing the wall deviation as a series of infinitesimal steps. We have also seen that the single loss for large steps is far higher for the round dielectric waveguide than it is for the slab waveguide. We might thus worry that the losses caused by random wall perturbations may also be far higher for the dominant mode of the round dielectric waveguide. Fortunately, this pessimistic expectation is not true. The radiation losses caused by wall roughness of the round dielectric rod are no worse than they are for the modes of the slab waveguide.

The random wall losses are treated on the basis of a statistical model. The correlation function describing the wall perturbation is assumed to be a simple exponential function that is characterized by two param-

eters, the rms deviation from perfect straightness A and the correlation length B .

Figure 9 shows a series of curves of the normalized relative radiation loss as a function of the ratio of correlation length to waveguide radius B/a for a guide with index of refraction $n = 1.432$ (teflon). The curve parameter is the product of vacuum propagation constant times waveguide radius, ka . Also shown for means of comparison is the loss of the circular electric mode of the round waveguide as a dotted line. It is apparent that the radiation losses of the dominant mode are approximately equal to the radiation loss of the circular electric mode. A comparison with the results of Ref. 1 shows that the losses of Fig. 9 are approximately four times as high as the corresponding losses for the slab waveguide. For a meaningful comparison we must remember, however, that the slab waveguide losses were computed under the assumption that only one of the two slab boundaries was randomly perturbed. It seems reasonable to compare the losses of the round rod to a slab waveguide whose two walls are perturbed in a correlated way. In fact, if we assume that the thickness of the slab waveguide changes in a manner that provides equal but opposite displacement of each side of the guide we would obtain a four times higher loss than is shown in the curves of Ref. 1. The agreement between the radiation losses of the

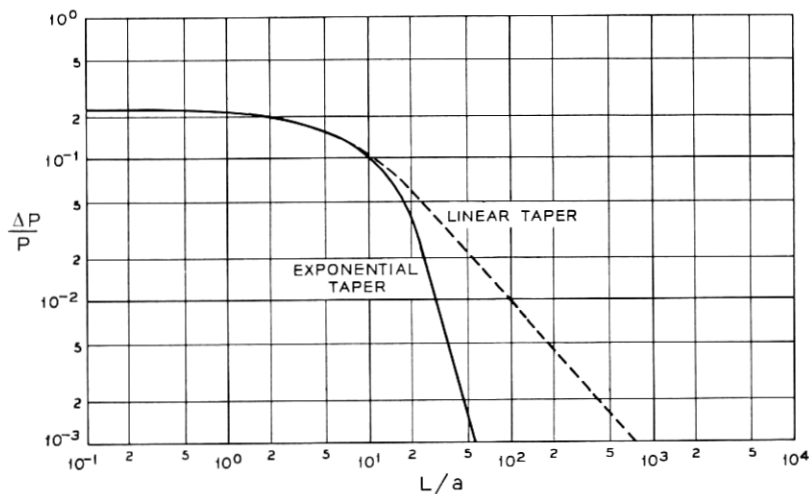


Fig. 8—Relative radiation loss of the linear (dashed line) and the exponential (solid line) taper. ($n = 1.432$, $a_2/a_1 = 0.5$, $ka_1 = 2.5$.)

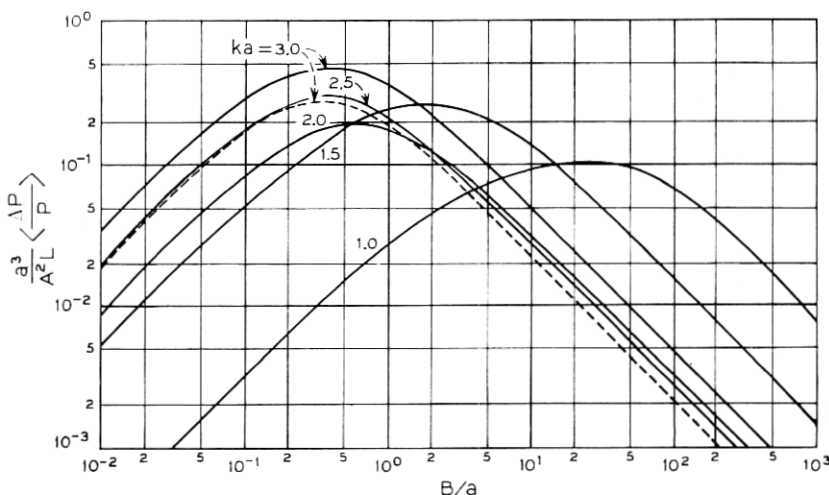


Fig. 9—Normalized radiation losses caused by random wall perturbations. The solid lines correspond to the dominant mode of the round guide, the dashed line represents the TE_{01} mode of this waveguide. ($n = 1.432$.) The curve parameters are the values of ka .

slab waveguide and the random wall losses of the round dielectric waveguide is quite close.

Figure 10 shows similar loss curves for a round waveguide with index of refraction $n = 1.01$. These curves too are about four times as high as the corresponding slab waveguide losses for the reason explained above. The curves of Fig. 10 are representative of the wall losses of a clad optical fiber with 1 percent index difference. As an example let us assume that we operate an optical fiber with a vacuum wavelength of $\lambda = 1 \mu\text{m}$. The value $ka = 15$ corresponds to a radius $a = 2.4 \mu\text{m}$ for the inner core of the fiber. If we assume that the correlation length of the exponential correlation function assumes its worst possible value $B/a = 2.0$, we find from Fig. 10 the normalized loss

$$\frac{a^3}{A^2 L} \frac{\Delta P}{P} = 0.04.$$

A loss factor of

$$\alpha = \frac{1}{L} \frac{\Delta P}{P} = 2.3 \text{ km}^{-1} = 10 \text{ dB/km}$$

would be caused by an rms deviation of the waveguide radius $= A \cdot 9 \cdot 10^{-8} \text{ cm} = 9 \text{ \AA}$. This example shows how very stringent the

tolerance requirements can be. In a realistic case there will not only be variations of the waveguide radius. In addition we do not know the statistical model of the correlation function that must be applied in each case. However, comparison of different correlation function models has shown that the peak and its location in Figs. 9 and 10 is not dependent on the assumed statistical model. The decay of the loss curves toward increasing values of B/a is strongly model dependent.

III. THEORY

3.1 The Dominant Guided Mode

The field components of an arbitrary guided mode in the waveguide are described by the following equations:⁵

$$E_z = A J_\nu(\kappa r) \cos \nu \phi \quad (3a)$$

$$H_z = B J_\nu(\kappa r) \sin \nu \phi \quad (3b)$$

$$E_r = -\frac{i}{\kappa^2} \left[\kappa \beta_0 A J'_\nu(\kappa r) + \omega \mu B \frac{\nu}{r} J_\nu(\kappa r) \right] \cos \nu \phi \quad (3c)$$

$$E_\phi = \frac{i}{\kappa^2} \left[\beta_0 A \frac{\nu}{r} J_\nu(\kappa r) + \kappa \omega \mu B J'_\nu(\kappa r) \right] \sin \nu \phi \quad (3d)$$

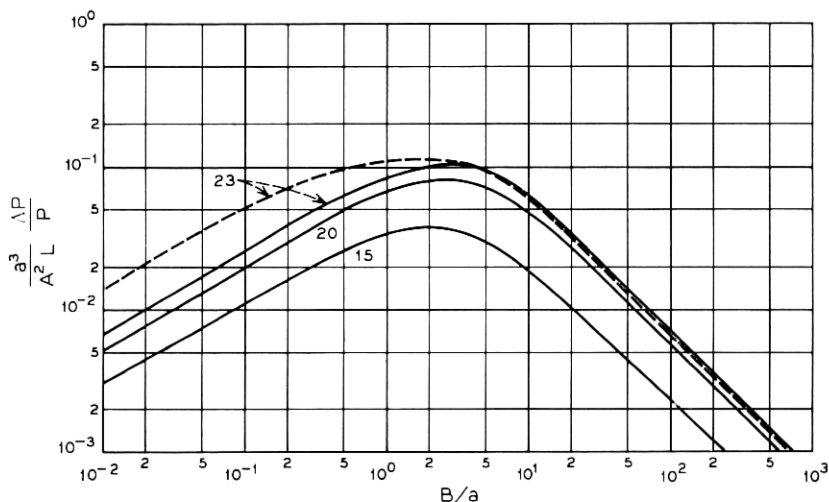


Fig. 10—These curves are similar to Fig. 9 with $n = 1.01$. The curve parameters are the values of ka .

$$H_r = -\frac{i}{\kappa^2} \left[n^2 \omega \epsilon_0 A \frac{\nu}{r} J_\nu(\kappa r) + \kappa \beta_0 B J'_\nu(\kappa r) \right] \sin \nu \phi \quad (3e)$$

$$H_\phi = -\frac{i}{\kappa^2} \left[n^2 \kappa \omega \epsilon_0 A J'_\nu(\kappa r) + \beta_0 B \frac{\nu}{r} J_\nu(\kappa r) \right] \cos \nu \phi. \quad (3f)$$

These equations describe the field inside of the round dielectric rod, $r \leq a$. The functions J_ν are the Bessel functions of order ν , a prime indicates the derivative with respect to the argument (not with respect to r). The parameter ν must be an integer in order to make sine and cosine periodic functions of the azimuth ϕ with period 2π . The factor

$$e^{i(\omega t - \beta_0 z)} \quad (4)$$

was omitted from equations (3). The propagation constant β_0 is related to the constants κ and the free space propagation constant k by the relations

$$k^2 = \omega^2 \epsilon_0 \mu_0 \quad (5)$$

and

$$\kappa^2 = n^2 k^2 - \beta_0^2, \quad (6)$$

where n is the index of refraction of the dielectric material. The constants A and B are not independent of each other. Their mutual dependence is given by the boundary conditions for the field components. The fields on the outside of the dielectric rod $r \geq a$ are given by the equations

$$E_z = CH_\nu^{(1)}(i\gamma r) \cos \nu \phi \quad (7a)$$

$$H_z = DH_\nu^{(1)}(i\gamma r) \sin \nu \phi \quad (7b)$$

$$E_r = \frac{i}{\gamma^2} \left[i\gamma \beta_0 CH_\nu^{(1)'}(i\gamma r) + \omega \mu D \frac{\nu}{r} H_\nu^{(1)}(i\gamma r) \right] \cos \nu \phi \quad (7c)$$

$$E_\phi = -\frac{i}{\gamma^2} \left[\beta_0 C \frac{\nu}{r} H_\nu^{(1)}(i\gamma r) + i\gamma \omega \mu DH_\nu^{(1)'}(i\gamma r) \right] \sin \nu \phi \quad (7d)$$

$$H_r = \frac{i}{\gamma^2} \left[\omega \epsilon_0 C \frac{\nu}{r} H_\nu^{(1)}(i\gamma r) + i\gamma \beta_0 DH_\nu^{(1)'}(i\gamma r) \right] \sin \nu \phi \quad (7e)$$

$$H_\phi = \frac{i}{\gamma^2} \left[i\gamma \omega \epsilon_0 CH_\nu^{(1)'}(i\gamma r) + \beta_0 D \frac{\nu}{r} H_\nu^{(1)}(i\gamma r) \right] \cos \nu \phi \quad (7f)$$

where $H_\nu^{(1)}$ is the Hankel function of order ν and of the first kind. The prime indicates again its derivative with respect to its argument. The

argument is imaginary in order to ensure that the field distribution decays exponentially at large distance from the rod. The time and z -dependent factor (4) has again been suppressed. The parameter γ is related to the propagation constant β_0 by the equation

$$\gamma^2 = \beta_0^2 - k^2.$$

The field components were written down quite generally for an arbitrary guided mode. The lowest order or dominant mode of the guide follows from these equations with

$$\nu = 1. \quad (8)$$

The following discussion will be limited to the special case $\nu = 1$. The connection between the amplitude coefficients and the determination of the propagation constant follows from the boundary conditions for the field components. The requirement that E_z , E_ϕ , H_z and H_ϕ are continuous at the boundary $r = a$ leads to the following eigenvalue equation for the determination of the propagation constant β_0 of the guided mode

$$\left\{ n^2 \frac{a\gamma^2}{\kappa} \left[\frac{J_0(\kappa a)}{J_1(\kappa a)} - \frac{1}{\kappa a} \right] + \left[\gamma a \frac{iH_0^{(1)}(i\gamma a)}{H_1^{(1)}(i\gamma a)} - 1 \right] \right\} \cdot \left\{ \frac{a\gamma^2}{\kappa} \left[\frac{J_0(\kappa a)}{J_1(\kappa a)} - \frac{1}{\kappa a} \right] + \left[\gamma a \frac{iH_0^{(1)}(i\gamma a)}{H_1^{(1)}(i\gamma a)} - 1 \right] \right\} = \left[(n^2 - 1) \frac{\beta_0 k}{\kappa^2} \right]^2. \quad (9)$$

A few numerical values obtained from (9) are shown in Table I. The

TABLE I—SOME NUMERICAL VALUES OF β_0

$n \simeq 1.432$ ($n^2 = 2.05$)		$n = 1.01$	
ka	$\beta_0 a$	ka	$\beta_0 a$
0.5	0.50000013	2.0	2.0000001
0.625	0.62500485	4.0	4.0000011
0.75	0.75006586	5.0	5.0000672
0.875	0.8758141	6.0	6.0006747
1.0	1.0043348	7.0	7.0026448
1.125	1.1387424	8.0	8.0064648
1.25	1.2816903	9.0	9.0121047
1.375	1.434524	10.0	10.019281
1.5	1.5970437	12.0	12.03695
1.75	1.9458015	14.0	14.057344
2.0	2.3149367	16.0	16.07916
2.25	2.6937751	18.0	18.101671
2.5	3.0761411	20.0	20.124481
2.75	3.458978	23.0	23.158808
3.0	3.8409082	24.0	24.170225
		27.0	27.204311

connection between the amplitude coefficients as a consequence of the boundary conditions is stated in the following equations:

$$B = -\left(\frac{\epsilon_0}{\mu_0}\right)^{\frac{1}{2}} \frac{(ka)(\kappa a)^2}{(\beta_0 a)\left(1 + \frac{\kappa^2}{\gamma^2}\right)} \cdot \left\{ \frac{n^2}{\kappa a} \left[\frac{J_0(\kappa a)}{J_1(\kappa a)} - \frac{1}{\kappa a} \right] + \frac{1}{\gamma a} \left[\frac{iH_0^{(1)}(i\gamma a)}{H_1^{(1)}(i\gamma a)} - \frac{1}{\gamma a} \right] \right\} A \quad (10)$$

$$C = \frac{J_1(\kappa a)}{H_1^{(1)}(i\gamma a)} A \quad (11)$$

$$D = \frac{J_1(\kappa a)}{H_1^{(1)}(i\gamma a)} B. \quad (12)$$

It is necessary to know the relation between the amplitude coefficients and the power P carried by the mode:

$$P = \frac{\pi}{4} \left[\frac{k\beta_0}{\kappa^4} \{ (a\kappa)^2 [J_0^2(\kappa a) + J_1^2(\kappa a)] - 2J_1^2(\kappa a) \} \left(n^2 + \frac{\mu_0}{\epsilon_0} \frac{B^2}{A^2} \right) + \frac{k\beta}{\gamma^4} \left\{ (a\gamma)^2 \left[\frac{H_0^{(1)2}(i\gamma a)}{H_1^{(1)2}(i\gamma a)} + 1 \right] + 2 \right\} J_1^2(\kappa a) \left(1 + \frac{\mu_0}{\epsilon_0} \frac{B^2}{A^2} \right) + 2 \left(\frac{\mu_0}{\epsilon_0} \right)^{\frac{1}{2}} \frac{B}{A} \left(\frac{\beta_0^2 + n^2 k^2}{\kappa^4} - \frac{\beta_0^2 + k^2}{\gamma^4} \right) J_1^2(\kappa a) \right] \left(\frac{\epsilon_0}{\mu_0} \right)^{\frac{1}{2}} A^2. \quad (13)$$

Equations (3) through (13) provide a complete description of the guided modes of symmetry $\cos \phi$. The lowest order solution of the eigenvalue equation (9) is the dominant mode of the round dielectric rod. This mode does not experience a cutoff. In principle it can be supported by any round dielectric rod of arbitrarily small cross section and arbitrarily low frequency. All other modes of the round dielectric waveguide exist only above their respective cutoff frequencies. All entries in Table I belong to single mode (with $\cos \phi$ symmetry) operation.

3.2 Radiation Modes of the Round Dielectric Rod

The number of guided modes that the round dielectric rod can support is finite at any given frequency. In order to obtain a complete set of normal modes of the structure we need to consider also the continuous spectrum of unguided modes.

Any solution of Maxwell's equations that satisfies the boundary condition is called a mode if its z -dependence (and time dependence) is given by equation (4). The guided modes are distinguished from the

unguided or radiation modes by the fact that their field distributions decay exponentially for increasing values of r outside of the waveguide. The radiation modes, on the other hand, extend to infinity. As their name indicates they are necessary to describe the radiation field outside (and inside) of the dielectric waveguide. Since there is no need to limit the functions describing the radiation modes to those that decay exponentially in the limit of large values of r we use a combination of Bessel and Neumann functions to express the unguided modes. However, we must require that the field remains finite on axis at $r = 0$. These considerations allow us to express the unguided solutions of Maxwell's equations as follows: For $r \leq a$

$$E_z = FJ_\nu(\sigma r) \cos \nu\phi \quad (14a)$$

$$H_z = GJ_\nu(\sigma r) \sin \nu\phi \quad (14b)$$

$$E_r = -\frac{i}{\sigma^2} \left\{ \sigma \beta F J'_\nu(\sigma r) + \omega \mu G \frac{\nu}{r} J_\nu(\sigma r) \right\} \cos \nu\phi \quad (14c)$$

$$E_\phi = \frac{i}{\sigma^2} \left[\beta F \frac{\nu}{r} J_\nu(\sigma r) + \sigma \omega \mu G J'_\nu(\sigma r) \right] \sin \nu\phi \quad (14d)$$

$$H_r = -\frac{i}{\sigma^2} \left[n^2 \omega \epsilon_0 F \frac{\nu}{r} J_\nu(\sigma r) + \sigma \beta G J'_\nu(\sigma r) \right] \sin \nu\phi \quad (14e)$$

$$H_\phi = -\frac{i}{\sigma^2} \left[n^2 \sigma \omega \epsilon_0 F J'_\nu(\sigma r) + \beta G \frac{\nu}{r} J_\nu(\sigma r) \right] \cos \nu\phi. \quad (14f)$$

There is now no restriction to the possible values that the propagation constant β can assume. The relation between β and σ is given by

$$\sigma^2 = n^2 k^2 - \beta^2. \quad (15)$$

The field outside of the dielectric rod, $r \geq a$, is given by

$$E_z = [HJ_\nu(\rho r) + IN_\nu(\rho r)] \cos \nu\phi \quad (16a)$$

$$H_z = [KJ_\nu(\rho r) + MN_\nu(\rho r)] \sin \nu\phi \quad (16b)$$

$$E_r = -\frac{i}{\rho^2} \left\{ \rho \beta [HJ'_\nu(\rho r) + IN'_\nu(\rho r)] + \omega \mu \frac{\nu}{r} [KJ_\nu(\rho r) + MN_\nu(\rho r)] \right\} \cos \nu\phi \quad (16c)$$

$$E_\phi = \frac{i}{\rho^2} \left\{ \beta \frac{\nu}{r} [HJ_\nu(\rho r) + IN_\nu(\rho r)] + \rho \omega \mu [KJ'_\nu(\rho r) + MN'_\nu(\rho r)] \right\} \sin \nu\phi \quad (16d)$$

$$H_r = -\frac{i}{\rho^2} \left\{ \omega \epsilon_0 \frac{\nu}{r} [HJ_\nu(\rho r) + IN_\nu(\rho r)] + \rho \beta [KJ'_\nu(\rho r) + MN'_\nu(\rho r)] \right\} \sin \nu \phi \quad (16e)$$

$$H_\phi = -\frac{i}{\rho^2} \left\{ \rho \omega \epsilon_0 [HJ'_\nu(\rho r) + IN'_\nu(\rho r)] + \beta \frac{\nu}{r} [KJ_\nu(\rho r) + MN_\nu(\rho r)] \right\} \cos \nu \phi \quad (16f)$$

with

$$\rho^2 = k^2 - \beta^2. \quad (17)$$

The Neumann functions N_ν are here expressed in the notation of Jahnke-Emde.⁴ The determination of the coefficients of the radiation modes is complicated by an interesting phenomenon. The boundary conditions provide us with four equations. However, there are six undetermined coefficients in the set of equations (14) and (16). Even allowing for the fact that the power of the mode can be chosen arbitrarily so that one coefficient must remain undetermined by the boundary conditions, we have still one more coefficient than the boundary conditions, combined with the requirement of total power carried by the mode, are able to determine. This situation means physically that the sets of equations (14) and (16) represent a superposition of two modes that could be taken apart. A similar situation would have arisen in the case of the slab waveguide had we not been careful to separate the modes into even and odd field distributions from the very beginning. The present structure does not lend itself to a natural separation of the modes into even and odd ones. However, the formal field expressions (14) and (16) do, nevertheless, represent a superposition of two possible sets of modes. One might try to take arbitrarily either the coefficient F or G appearing in equation (14) equal to zero to try to separate out the two sets of modes. This procedure is mathematically beyond reproach but it suffers from a practical inconvenience. The resulting sets of modes would not be orthogonal. It is very desirable to choose the modes in such a way that they are all mutually orthogonal to each other. It is therefore necessary to determine the coefficients in a way that assures the orthogonality of all the modes. The boundary conditions combined with the requirement of mode orthogonality and a certain amount of power carried by each mode are still not enough to assure a unique solution of our problem. This is not surprising since it is always

possible to combine two arbitrary vectors in an infinite number of ways into two mutually orthogonal vectors.

The boundary conditions alone yield the following relations between the coefficients

$$H = \frac{\pi}{2} (\rho a) \left\{ \left[J_v(\sigma a) N'_v(\rho a) - n^2 \frac{\rho}{\sigma} J'_v(\sigma a) N_v(\rho a) \right] F + \frac{(n^2 - 1)k^2}{\rho \sigma^2 \omega \epsilon_0} \beta \frac{\nu}{a} J_v(\sigma a) N_v(\rho a) G \right\} \quad (18)$$

$$I = \frac{\pi}{2} (\rho a) \left\{ \left[n^2 \frac{\rho}{\sigma} J'_v(\sigma a) J_v(\rho a) - J_v(\sigma a) J'_v(\rho a) \right] F - \frac{(n^2 - 1)k^2}{\rho \sigma^2 \omega \epsilon_0} \beta \frac{\nu}{a} J_v(\sigma a) J_v(\rho a) G \right\} \quad (19)$$

$$K = \frac{\pi}{2} (\rho a) \left\{ \frac{(n^2 - 1)k^2}{\rho \sigma^2 \omega \mu} \beta \frac{\nu}{a} J_v(\sigma a) N_v(\rho a) F + \left[J_v(\sigma a) N'_v(\rho a) - \frac{\rho}{\sigma} J'_v(\sigma a) N_v(\rho a) \right] G \right\} \quad (20)$$

$$M = \frac{\pi}{2} (\rho a) \left\{ -\frac{(n^2 - 1)k^2}{\rho \sigma^2 \omega \mu} \beta \frac{\nu}{a} J_v(\sigma a) J_v(\rho a) F + \left[\frac{\rho}{\sigma} J'_v(\sigma a) J_v(\rho a) - J_v(\sigma a) J'_v(\rho a) \right] G \right\}. \quad (21)$$

Equations (14), (16) and (18) through (21) are sufficient to satisfy Maxwell's equations and the boundary conditions. The coefficients F and G are, so far, completely arbitrary. We consider now two sets of radiation modes. The first set is distinguished by using the coefficients with subscripts F_1 and G_1 while the coefficients of the second set are designated by F_2 and G_2 . The two sets of coefficients must now be adjusted to render the two sets of modes orthogonal. One of the infinitely many solutions of this problem is

$$\frac{F_2}{G_2} = -\frac{F_1}{G_1}. \quad (22)$$

The ratio of F_1/G_1 is now no longer arbitrary but is given by

$$\frac{F_1}{G_1} = \left(\frac{\mu_0}{\epsilon_0} \right)^{\frac{1}{2}} \left[\frac{(g - b)^2 + (e - d)^2 + (c^2 + f^2)}{(g - n^2 b)^2 + (e - n^2 d)^2 + (c^2 + f^2)} \right]^{\frac{1}{2}} \quad (23a)$$

with

$$b = \frac{\rho}{\sigma} J_1'(\sigma a) N_1(\rho a) \quad (23b)$$

$$c = \frac{(n^2 - 1)k}{\rho\sigma^2} \frac{\beta}{a} J_1(\sigma a) N_1(\rho a) \quad (23c)$$

$$d = \frac{\rho}{\sigma} J_1'(\sigma a) J_1(\rho a) \quad (23d)$$

$$e = J_1(\sigma a) J_1'(\rho a) \quad (23e)$$

$$f = \frac{(n^2 - 1)k}{\rho\sigma^2} \frac{\beta}{a} J_1(\sigma a) J_1(\rho a) \quad (23f)$$

$$g = J_1(\sigma a) N_1'(\rho a). \quad (23g)$$

Equation (23) was already specialized to the mode of symmetry $\cos \phi$, taking $\nu = 1$. The power carried by the radiation modes is given by

$$P = \left(\frac{\pi}{2}\right)^3 \frac{a^2 \beta}{\rho} \omega \epsilon_0 \left\{ \left[(g - n^2 b) + c \left(\frac{\mu_0}{\epsilon_0}\right)^{\frac{1}{2}} \frac{G}{F} \right]^2 + \left[(e - n^2 d) + f \left(\frac{\mu_0}{\epsilon_0}\right)^{\frac{1}{2}} \frac{G}{F} \right]^2 \right. \\ \left. + \left[c + (g - b) \left(\frac{\mu_0}{\epsilon_0}\right)^{\frac{1}{2}} \frac{G}{F} \right]^2 + \left[f + (e - d) \left(\frac{\mu_0}{\epsilon_0}\right)^{\frac{1}{2}} \frac{G}{F} \right]^2 \right\} F^2. \quad (24)$$

The normalization of the radiation modes involves the delta function in the same way as it did in the case of the slab waveguides.

3.3 Radiation Losses Caused by a Step

It has been shown previously³ that the radiation losses of arbitrary deformations of dielectric waveguides can be calculated from the knowledge of the radiation loss of a step. For simplicity we limit the discussion to waveguide imperfections that do not violate the condition (2). Condition (2) restricts the waveguide deformations to symmetrical changes of the waveguide diameter. More general deformations are far more difficult to calculate.

A step in the round dielectric rod is shown in Fig. 1. We restrict ourselves to a dominant mode waveguide. The radius of the larger part of the waveguide must be small enough to ensure that only the dominant mode of the structure can propagate. Waveguides with larger radii suffer conversion losses to other guided modes in addition to the radiation losses. Such losses have been studied for the case of the slab waveguide¹ and for circular electric modes in round dielectric waveguides.²

The radiation field can be expressed as an integral over all the radia-

tion modes. Indicating the modes by script letters with the superscript i for the incident guided mode, r for the reflected guided and radiation modes and t for the transmitted guided and radiation modes we can write the boundary condition at the step as follows:

$$\begin{aligned} \mathcal{E}_r^{(i)} + a_r \mathcal{E}_r^{(r)} + \int_0^\infty [q_r(\rho) \mathcal{E}_{r_1}^{(r)}(\rho) + p_r(\rho) \mathcal{E}_{r_2}^{(r)}(\rho)] d\rho \\ = c_i \mathcal{E}_r^{(t)} + \int_0^\infty [q_t(\rho) \mathcal{E}_{r_1}^{(t)}(\rho) + p_t(\rho) \mathcal{E}_{r_2}^{(t)}(\rho)] d\rho \end{aligned} \quad (25)$$

$$\begin{aligned} \mathcal{E}_\phi^{(i)} + a_r \mathcal{E}_\phi^{(r)} + \int_0^\infty [q_r(\rho) \mathcal{E}_{\phi_1}^{(r)}(\rho) + p_r(\rho) \mathcal{E}_{\phi_2}^{(r)}(\rho)] d\rho \\ = c_i \mathcal{E}_\phi^{(t)} + \int_0^\infty [q_t(\rho) \mathcal{E}_{\phi_1}^{(t)}(\rho) + p_t(\rho) \mathcal{E}_{\phi_2}^{(t)}(\rho)] d\rho \end{aligned} \quad (26)$$

$$\begin{aligned} \mathcal{H}_r^{(i)} + a_r \mathcal{H}_r^{(r)} + \int_0^\infty [q_r(\rho) \mathcal{H}_{r_1}^{(r)}(\rho) + p_r(\rho) \mathcal{H}_{r_2}^{(r)}(\rho)] d\rho \\ = c_i \mathcal{H}_r^{(t)} + \int_0^\infty [q_t(\rho) \mathcal{H}_{r_1}^{(t)}(\rho) + p_t(\rho) \mathcal{H}_{r_2}^{(t)}(\rho)] d\rho \end{aligned} \quad (27)$$

$$\begin{aligned} \mathcal{H}_\phi^{(i)} + a_r \mathcal{H}_\phi^{(r)} + \int_0^\infty [q_r(\rho) \mathcal{H}_{\phi_1}^{(r)}(\rho) + p_r(\rho) \mathcal{H}_{\phi_2}^{(r)}(\rho)] d\rho \\ = c_i \mathcal{H}_\phi^{(t)} + \int_0^\infty [q_t(\rho) \mathcal{H}_{\phi_1}^{(t)}(\rho) + p_t(\rho) \mathcal{H}_{\phi_2}^{(t)}(\rho)] d\rho. \end{aligned} \quad (28)$$

These equations express the continuity of the transverse electric and magnetic field components at the step. The field components that are shown to be functions of ρ belong to radiation modes while field components that are not explicitly indicated as functions of ρ belong to the dominant guided mode. The amplitude of the incident guided mode is unity. The approximate solution of the equation system (25) through (28) follows the same reasoning that was presented for the case of the slab waveguide.³ The coefficient c_i can be calculated by using the orthogonality of the waveguide modes to the right of the step. The modes to the right of the step are not orthogonal to the modes to the left of the step because of the different waveguide size. It is thus not possible to separate the coefficients q_r and p_r (which, incidentally, belong to the two orthogonal sets of radiation modes) from the coefficient a_r of the reflected guided mode. This problem makes it impossible to obtain an exact solution of the equation system. We neglect the reflected radiation modes when we calculate the coefficient c_i . This approximation is

justified by the fact that for large steps the radiation favors the forward direction so that q_r and p_r can be assumed to be small. For very small steps where the ratio of forward to backward scattered power can be expected to be more nearly unity we need not worry about the coefficients of the reflected radiation modes since the modes of the two guide sections become more nearly orthogonal to each other.

The transmission and reflection coefficients can thus be determined approximately with the result

$$c_t = \frac{2I_1 I_2}{(I_1 + I_2)P} \quad (29)$$

and

$$a_r = \frac{I_1 - I_2}{I_1 + I_2} \quad (30)$$

with

$$\begin{aligned} I_1 = & \frac{\pi}{2} \left\{ \frac{1}{\gamma_2^2} (\beta_1 A_1 - \omega \mu B_1) (\omega \epsilon_0 A_2 - \beta_2 B_2) \frac{J_1(\kappa_2 a_2)}{H_1^{(1)}(i\gamma_2 a_2)} \right. \\ & \cdot \left[\left(\frac{1}{\kappa_1^2} + \frac{1}{\gamma_1^2} \right) J_1(\kappa_1 a_1) H_1^{(1)}(i\gamma_2 a_1) - \frac{1}{\kappa_1^2} J_1(\kappa_1 a_2) H_1^{(1)}(i\gamma_2 a_2) \right] \\ & - \frac{1}{\kappa_1^2 \kappa_2^2} (\beta_1 A_1 - \omega \mu B_1) (n^2 \omega \epsilon_0 A_2 - \beta_2 B_2) J_1(\kappa_1 a_2) J_1(\kappa_2 a_2) \\ & + \frac{a_2}{\kappa_1 \kappa_2 (\frac{2}{\kappa_1^2} - \kappa_2^2)} (\omega \epsilon_0 n^2 \beta_1 A_1 A_2 + \omega \mu \beta_2 B_1 B_2) \\ & \cdot [\kappa_1 J_1(\kappa_1 a_2) J_0(\kappa_2 a_2) - \kappa_2 J_0(\kappa_1 a_2) J_1(\kappa_2 a_2)] \\ & + \frac{1}{\gamma_2} (\omega \epsilon_0 \beta_1 A_1 A_2 + \omega \mu \beta_2 B_1 B_2) \frac{J_1(\kappa_2 a_2)}{H_1^{(1)}(i\gamma_2 a_2)} \\ & \cdot \left[\frac{1}{\kappa_1^2 + \gamma_2^2} \left(i a_2 J_1(\kappa_1 a_2) H_0^{(1)}(i\gamma_2 a_2) - i a_1 J_1(\kappa_1 a_1) H_0^{(1)}(i\gamma_2 a_1) \right. \right. \\ & \left. \left. + \frac{\gamma_2}{\kappa_1} [a_2 J_0(\kappa_1 a_2) H_1^{(1)}(i\gamma_2 a_2) - a_1 J_0(\kappa_1 a_1) H_1^{(1)}(i\gamma_2 a_1)] \right) \right. \\ & \left. + \frac{a_1}{\gamma_2^2 - \gamma_1^2} \frac{J_1(\kappa_1 a_1)}{H_1^{(1)}(i\gamma_1 a_1)} \left(i H_1^{(1)}(i\gamma_1 a_1) H_0^{(1)}(i\gamma_2 a_1) \right. \right. \\ & \left. \left. - i \frac{\gamma_2}{\gamma_1} H_0^{(1)}(i\gamma_1 a_1) H_1^{(1)}(i\gamma_2 a_1) \right) \right] \Bigg\} \quad (31) \end{aligned}$$

and with

$$\begin{aligned}
 I_2 = & \frac{\pi}{2} \left\{ -\frac{1}{\kappa_1^2} (n^2 \omega \epsilon_0 A_1 - \beta_1 B_1) (\beta_2 A_2 - \omega \mu B_2) \frac{J_1(\kappa_2 a_2)}{H_1^{(1)}(i\gamma_2 a_2)} \right. \\
 & \cdot \left[\left(\frac{1}{\kappa_2^2} + \frac{1}{\gamma_2^2} \right) J_1(\kappa_1 a_2) H_1^{(1)}(i\gamma_2 a_2) - \frac{1}{\gamma_2^2} J_1(\kappa_1 a_1) H_1^{(1)}(i\gamma_2 a_1) \right] \\
 & + \frac{1}{\gamma_1 \gamma_2^2} (\omega \epsilon_0 A_1 - \beta_1 B_1) (\beta_2 A_2 - \omega \mu B_2) \frac{J_1(\kappa_2 a_2)}{H_1^{(1)}(i\gamma_2 a_2)} J_1(\kappa_1 a_1) H_1^{(1)}(i\gamma_2 a_1) \\
 & + \frac{a_1}{\gamma_1 \gamma_2 (\gamma_2^2 - \gamma_1^2)} (\omega \epsilon_0 \beta_2 A_1 A_2 + \omega \mu \beta_1 B_1 B_2) \frac{J_1(\kappa_1 a_1)}{H_1^{(1)}(i\gamma_1 a_1)} \frac{J_1(\kappa_2 a_2)}{H_1^{(1)}(i\gamma_2 a_1)} \\
 & \cdot [i\gamma_1 H_1^{(1)}(i\gamma_1 a_1) H_0^{(1)}(i\gamma_2 a_1) - i\gamma_2 H_0^{(1)}(i\gamma_1 a_1) H_1^{(1)}(i\gamma_2 a_1)] \\
 & + \frac{1}{\kappa_1} (n^2 \omega \epsilon_0 \beta_2 A_1 A_2 + \omega \mu \beta_1 B_1 B_2) \\
 & \cdot \left[\frac{a_2}{\kappa_1^2 - \kappa_2^2} \left(\frac{\kappa_1}{\kappa_2} J_1(\kappa_1 a_2) J_0(\kappa_2 a_2) - J_0(\kappa_1 a_2) J_1(\kappa_2 a_2) \right) \right. \\
 & + \frac{1}{\kappa_1^2 + \gamma_2^2} \frac{J_1(\kappa_2 a_2)}{H_1^{(1)}(i\gamma_2 a_2)} \left(a_2 J_0(\kappa_1 a_2) H_1^{(1)}(i\gamma_2 a_2) - a_1 J_0(\kappa_1 a_1) H_1^{(1)}(i\gamma_2 a_1) \right. \\
 & \left. \left. + \frac{\kappa_1}{\gamma_2} [ia_2 J_1(\kappa_1 a_2) H_0^{(1)}(i\gamma_2 a_2) - ia_1 J_1(\kappa_1 a_1) H_0^{(1)}(i\gamma_2 a_1)] \right) \right] \Bigg\}. \quad (32)
 \end{aligned}$$

The indices 1 and 2 attached to the coefficients and parameters indicate that the corresponding quantities belong to the waveguide to the left of the step (index 1) or to the right of the step (index 2). The coefficients A and B are the amplitude coefficients introduced in equations (3), (10) and (13). The factor P in equation (29) is the power carried by the incident guided mode. It was assumed that the power of all the modes is identical. The actual power carried by the mode is accounted for by the expansion coefficients a_r , q_r , p_r , q_t , p_t , and c_t . The power coefficients appearing in equations (13) and (29) are also identical.

The theory of the dominant mode of the round dielectric waveguide is far more complex than the corresponding theory of the slab waveguide. This explains why the slab waveguide is so much more convenient to use for studying the general properties of radiation losses.

The radiation loss caused by the step is obtained from

$$\frac{\Delta P}{P} = 1 - |c_t|^2 - |a_r|^2. \quad (33)$$

However, the same radiation loss can also be obtained by accounting

for the power carried away in the radiation modes. We can therefore write also

$$\frac{\Delta P}{P} = \int_{-k}^k (|q|^2 + |p|^2) \frac{|\beta|}{\rho} d\beta. \quad (34)$$

The subscripts r and t have been dropped from the expansion coefficients p and q . Both reflected and transmitted radiation modes are automatically included by extending the integration range from $-k$ to k so that backward as well as forward traveling waves are included. The factor $|\beta|/\rho$ appearing under the integration sign arose from converting the integration variable ρ to β .

The theory becomes much simpler when we limit the derivation of the p and q coefficients to small steps. It was shown in the work on slab waveguides³ that arbitrary deformations of the waveguide wall can be treated as a succession of small steps. Even abrupt tapers can be described this way. In the limit of small step height Δa we can write

$$\Delta a = \frac{da}{dz} \Delta z. \quad (35)$$

The expansion coefficients q_r and q_t can approximately be obtained from equations (25) through (28) by a method that has been explained in some detail in Ref. 3.

$$q(\rho) = \int_0^L I(\rho, z) \frac{da}{dz} e^{-i \int_0^z (\beta_0 - \beta) dz} dz. \quad (36)$$

The subscript r or t of q is no longer necessary since q_r corresponds to negative values of β while q_t corresponds to positive values of β . The derivation of q has been simplified by expressing quantities pertaining to the waveguide to the right of the step in terms of the corresponding quantities for the waveguide to the left of the step. This approximation involves an expansion of the field quantities in Taylor series keeping only the first two terms of the expansion

$$F(a_2) = F(a_1) + \left(\frac{\partial F}{\partial a} \right)_{a=a_1} \Delta a. \quad (37)$$

The orthogonality of the modes belonging to the same section of waveguide can be employed to eliminate many terms from the expressions. The resulting expressions for $I(\rho, z)$ is far simpler than it would be had we considered a large step. We obtain

$$\begin{aligned}
I(\rho, z) = & \frac{\pi}{4\rho^2\gamma^2P} J_1(\kappa a) \\
& \cdot \left\{ (\beta_0 + \beta)\gamma\rho \left(\omega\epsilon_0 A \frac{\partial H}{\partial a} + \omega\mu B \frac{\partial K}{\partial a} \right) \right. \\
& \cdot \left[a \frac{\gamma J_0(\rho a) + i\rho \frac{H_0^{(1)}(i\gamma a)}{H_1^{(1)}(i\gamma a)} J_1(\rho a)}{\gamma^2 + \rho^2} - \frac{1}{\gamma\rho} J_1(\rho a) \right] \\
& + (\beta_0 + \beta)\gamma\rho \left(\omega\epsilon_0 A \frac{\partial I}{\partial a} + \omega\mu B \frac{\partial M}{\partial a} \right) \\
& \cdot \left[a \frac{\gamma N_0(\rho a) + i\rho \frac{H_0^{(1)}(i\gamma a)}{H_1^{(1)}(i\gamma a)} N_1(\rho a)}{\gamma^2 + \rho^2} - \frac{1}{\gamma\rho} N_1(\rho a) \right] \\
& + (k^2 + \beta_0\beta) \left[\left(A \frac{\partial K}{\partial a} + B \frac{\partial H}{\partial a} \right) J_1(\rho a) \right. \\
& \left. \left. + \left(A \frac{\partial M}{\partial a} + B \frac{\partial I}{\partial a} \right) N_1(\rho a) \right] \right\}. \quad (38)
\end{aligned}$$

The derivatives of the amplitude coefficients H , I , K , and M of equations (18) through (21) are taken by keeping F and G constant. The reason for this prescription is the fact that the terms containing derivatives of F and G disappear from the equations because of mode orthogonality.

$$\begin{aligned}
\frac{\partial H}{\partial a} = & \frac{\pi\rho}{2} \left[\left\{ a \frac{\sigma^2 - n^2\rho^2}{\sigma} J_0(\sigma a) \left[N_0(\rho a) - \frac{1}{\rho a} N_1(\rho a) \right] \right. \right. \\
& + \left[\frac{2}{\rho a} - \rho a + n^2 \left(\rho a - \frac{2\rho}{a\sigma^2} \right) \right] J_1(\sigma a) N_1(\rho a) \\
& + \left(n^2 \frac{\rho^2}{\sigma^2} - 1 \right) J_1(\sigma a) N_0(\rho a) \left. \right\} F + \frac{(n^2 - 1)k^2\beta}{\omega\epsilon_0\rho\sigma^2} \\
& \cdot \left\{ \sigma J_0(\sigma a) N_1(\rho a) + \rho J_1(\sigma a) N_0(\rho a) - \frac{2}{a} J_1(\sigma a) N_1(\rho a) \right\} G \quad (39) \\
\frac{\partial I}{\partial a} = & -\frac{\pi\rho}{2} \left[\left\{ a \frac{\sigma^2 - n^2\rho^2}{\sigma} J_0(\sigma a) \left[J_0(\rho a) - \frac{1}{\rho a} J_1(\rho a) \right] \right. \right.
\end{aligned}$$

$$\begin{aligned}
& + \left[\frac{2}{\rho a} - \rho a + n^2 \left(\rho a - \frac{2\rho}{a\sigma^2} \right) \right] J_1(\sigma a) J_1(\rho a) \\
& + \left(n^2 \frac{\rho^2}{\sigma^2} - 1 \right) J_1(\sigma a) J_0(\rho a) \Big\} F + \frac{(n^2 - 1)k^2 \beta}{\omega \epsilon_0 \rho \sigma^2} \\
& \cdot \left\{ \sigma J_0(\sigma a) J_1(\rho a) + \rho J_1(\sigma a) J_0(\rho a) - \frac{2}{a} J_1(\sigma a) J_1(\rho a) \right\} G \Big] \quad (40)
\end{aligned}$$

$$\begin{aligned}
\frac{\partial K}{\partial a} &= \frac{\pi \rho}{2\sigma} (n^2 - 1)k^2 \\
& \cdot \left[\frac{\beta}{\omega \mu \sigma \rho} \left\{ \sigma J_0(\sigma a) N_1(\rho a) + \rho J_1(\sigma a) N_0(\rho a) - \frac{2}{a} J_1(\sigma a) N_1(\rho a) \right\} F \right. \\
& + \left\{ a J_0(\sigma a) \left[N_0(\rho a) - \frac{1}{\rho a} N_1(\rho a) \right] \right. \\
& + \left. \left. \frac{2}{\rho \sigma a} J_1(\sigma a) N_1(\rho a) - \frac{1}{\sigma} J_1(\sigma a) N_0(\rho a) \right\} G \right] \quad (41)
\end{aligned}$$

$$\begin{aligned}
\frac{\partial M}{\partial a} &= -\frac{\pi \rho}{2\sigma} (n^2 - 1)k^2 \\
& \cdot \left[\frac{\beta}{\omega \mu \sigma \rho} \left\{ \sigma J_0(\sigma a) J_1(\rho a) + \rho J_1(\sigma a) J_0(\rho a) - \frac{2}{a} J_1(\sigma a) J_1(\rho a) \right\} F \right. \\
& + \left\{ a J_0(\sigma a) \left[J_0(\rho a) - \frac{1}{\rho a} J_1(\rho a) \right] \right. \\
& + \left. \left. \frac{2}{\rho \sigma a} J_1(\sigma a) J_1(\rho a) - \frac{1}{\sigma} J_1(\sigma a) J_0(\rho a) \right\} G \right] \quad (42)
\end{aligned}$$

Equation (36) holds for q as well as for p . It is only necessary to insert F_1 and G_1 in equations (38) through (42) to obtain the q coefficients while the p coefficients are obtained by replacing F_1 , G_1 with F_2 , G_2 .

In order to use equation (34) for the relative power loss caused by radiation, it is necessary to calculate q and p with the help of equations (36) and (38). The coefficients appearing in these equations must be obtained from equations (39) through (42), and (10), (13), (22), (23), and (24). It should be apparent that this theory is of considerable complexity and can be handled only on an electronic computer. It is sad that the dominant mode in a round dielectric waveguide leads to such a complicated theory in comparison with the simple treatment of the slab waveguide.

3.4 Random Wall Perturbations

An important source of loss is the radiation that is caused by small random perturbations of the waveguide wall. Such radiation losses have been discussed for slab waveguides in Ref. 1 and for round dielectric waveguides operating with the circular electric guided mode in Ref. 2. Equation (36) of our present analysis can be used to calculate the loss of the dominant mode of the round waveguide caused by random wall perturbations. Since the step losses of the dominant mode of the round waveguide are so much higher than the corresponding losses of TE and TM modes of the slab waveguide one might fear that the losses caused by infinitesimal random perturbations of the waveguide wall may also be substantially higher. Fortunately, this is not the case. The losses caused by random wall perturbations are of the same order of magnitude for all types of dielectric waveguides that have been studied so far.

The losses caused by random wall perturbations are calculated with the help of a statistical model. Instead of using equation (34) for a particular waveguide we form the ensemble average $\langle \Delta P/P \rangle$ over many statistically similar systems. For very slight perturbations of the waveguide wall we can assume that $I(\rho, z)$ is independent of the z coordinate and write equation (36), after a partial integration, in the form

$$q(\rho) = +i(\beta_0 - \beta)I(\rho) \int_0^L a(z)e^{-i(\beta_0 - \beta)z} dz. \quad (43)$$

The argument z has been dropped from $I(\rho)$ since this function is no longer dependent on z . The partial integration had the beneficial effect of causing $a(z)$ instead of its derivative to appear under the integration sign. It was shown in Ref. 1 how substitution of equation (43) in (34) makes the scattering loss dependent on the correlation function

$$R(u) = \langle a(z)a(z-u) \rangle \quad (44)$$

after the expectation value has been taken. It is, therefore, possible to write the average value of the relative radiation loss as

$$\left\langle \frac{\Delta P}{P} \right\rangle = 2L \int_{-\infty}^{\infty} (\beta_0 - \beta)^2 [|I^{(1)}(\rho)|^2 + |I^{(2)}(\rho)|^2] F(\beta) \frac{|\beta|}{\rho} d\beta \quad (45)$$

with

$$F(\beta) = \int_0^{\infty} R(u) \cos(\beta_0 - \beta)u du. \quad (46)$$

The superscripts 1 and 2 indicate that the function $I(\rho)$ has been com-

puted for both types of radiation modes that are associated with F_1 , G_1 and F_2 , G_2 .

If we use for the correlation function a simple exponential function

$$R(u) = A^2 \exp\left(-\frac{|u|}{B}\right), \quad (47)$$

$F(\beta)$ specializes to¹

$$F(\beta) = \frac{A^2}{B \left[(\beta_0 - \beta)^2 + \frac{1}{B^2} \right]}. \quad (48)$$

IV. CONCLUSION

We have found that the radiation losses of the dominant mode of a round dielectric waveguide are much higher than the corresponding losses of TE and TM modes of the slab waveguide. The radiation losses of the dominant mode of the round dielectric waveguide with an abrupt step have been verified by a millimeter wave experiment. The step losses of a ribbon waveguide were also measured and found to lie between the losses of the dominant mode of the round waveguide and the TE mode losses of the slab waveguide, but closer to the latter. It is thus apparent that the slab waveguide can tolerate abrupt steps exceptionally well.

The radiation loss of a tapered round waveguide can be minimized by using a gentle taper instead of an abrupt step to accomplish the change of the waveguide radius. The losses of a linear taper are only slightly higher than the losses of a taper that was designed to equalize the loss contributions from different parts of the taper. It appears, therefore, that the design of optimum tapers is not profitable compared to their greater mechanical complexity.

The losses caused by slight random wall imperfections are very similar for the dominant mode and the circular electric TE_{01} mode of the round dielectric rod as well as the TE and TM modes of the dielectric slab waveguide. This result is surprising since the step losses of the dominant mode of the round waveguide are so much higher than the step losses of the slab waveguide. However, this result shows that the radiation losses caused by slight random wall perturbations can be studied with the help of the simple model of the slab waveguide and the results so obtained can be used to evaluate the performance of round dielectric waveguides.

REFERENCES

1. Marcuse, D., "Mode Conversion Caused by Surface Imperfections of a Dielectric Slab Waveguide," B.S.T.J., 48, No. 10 (December 1969), pp. 3177-3215.
2. Marcuse, D., and Derosier, R. M., "Mode Conversion Caused by Diameter Changes of a Round Dielectric Waveguide," B.S.T.J., 48, No. 10 (December 1969), pp. 3217-3232.
3. Marcuse, D., "Radiation Losses of Tapered Dielectric Slab Waveguides," B.S.T.J., 49, No. 2 (February 1970), pp. 273-290 and 49, No. 5 (May-June 1970), p. 919.
4. Jahnke, E., and Emde, F., *Tables of Functions*, New York: Dover, 1945.
5. Collin, R.E., "Field Theory of Guided Waves," New York: McGraw-Hill, 1960.
6. Snyder, A. W., "Coupling of Modes on a Tapered Dielectric Cylinder," IEEE Trans. Microwave Theory and Techniques, 18, No. 7 (July 1970), pp. 383-392.
7. Snyder, A. W., "Radiation Losses due to Variations of Radius on Dielectric or Optical Fibres," IEEE Trans. Microwave Theory and Techniques, 18, No. 9 (September 1970).

